Title: Property Enhancement of Cast Iron to be Used for Nuclear Cask

Authors:

B.P.MAHTO

M.Tech (Steel Technology),

Department of Metallurgical and Materials Engineering,

National Institute of Technology Rourkela, Odisha, India-769008

Dr. S.C.MISHRA

Professor,

Department of Metallurgical and Materials Engineering,

National Institute of Technology Rourkela, Odisha, India-769008

Dr. S.SEN

Associate Professor,

Department of Metallurgical and Materials Engineering,

National Institute of Technology Rourkela, Odisha, India-769008

Shri J.S.DUBEY

Post Irradiation Division,

Bhaba Atomic Research Centre, Mumbai, India-400085

R.K.BEHERA*

Ph.D Scholar,

Department of Metallurgical and Materials Engineering,

National Institute of Technology Rourkela, Odisha, India-769008

*Corresponding author's E-mail: funnyranjan.1986@gmail.com

Contact no.: +918895871603

Property Enhancement of Cast Iron to be Used for Nuclear Cask

R.K.BEHERA[1]*, B.P.MAHTO[1], J.S.DUBEY[2], S.C.MISHRA[1], S.SEN[1]

Department of Metallurgical and Materials Engineering,

[1]National Institute of Technology Rourkela, Odisha, India-769008

[2]Bhaba Atomic Research Centre (Post Irradiation Examination Division), Mumbai, India-400085

*Corresponding author's E-mail: funnyranjan.1986@gmail.com

Abstract

Ductile iron (DI) is the most preferable material which finds its application in various structural, automotive and engineering fields due to the excellent combination of strength, toughness and ductility. The current investigation enlightens the relation between morphological aspects of ductile iron with its mechanical properties to be used for safety prospectus in nuclear industry. Ductile iron specimens with varying alloying elements are subjected to annealing and austempering heat treatment processes. Faster cooling rate appeared to increase the nodule count in austempered specimens compensating the nodularity value, subsequently decrease in ductility and impact strength. The ductility and impact energy value for annealed specimens are observed to be increasing with the increase in ferrite area fraction and nodularity, whereas the increased amount of Ni & Cr results in increase of hardness via solid solution strengthening. Austempered specimens are found to have stronger than annealed specimens and failed in somewhat brittle manner characterized by river pattern, whereas ductile failure mode is characterized by presence of dimples in latter case has been observed.

Keywords: ferritic ductile iron, nodularity, UTS, Vickers hardness, impact energy, failure phenomena

1.   Introduction

Spheroidal graphite cast iron (SGCI)/ ductile iron is being used in many industrial applications due to its versatile mechanical properties as compared to other cast irons and steel. Although it has good mechanical properties in as cast condition; efforts are being made to enhance the properties through various heat treatment processes by transforming the as cast ferritic or pearlitic matrix into bainitic, martensitic and dual matrix (martensite + ferrite) structures [1-5]. The austempering treatment produces a matrix of lower acicular bainite or coarse upper bainite depending on the transformation temperature and time. Austempering involves isothermal transformation of primary austenite (γ_0) into acicular ferrite (α) and carbon enriched stable austenite (γ_c) resulting ausferritic matrix structure. This ausferritic matrix may have supplemental martensite, carbide, pearlite and retained austenite content for an austempering temperature range of 250°C-350°C, resulting high strength with lower toughness. However with increase in austempering time more than 2hr the retained austenite disappears from the matrix resulting increased static as well as dynamic toughness [6-12]. Furthermore it is well reported in the literature [13-16] that with increasing austempering temperature above 350°C and austempering time more than 2hr only ferrite (α) and carbon enriched stable austenite (γ_c) were present. However for temperatures above 350°C at lower time; traces of retained austenite may be present. The resulting matrix at higher austempering temperature comprises coarser ferrite and austenite leading to coarse upper bainitic matrix causing considerable strength level along with increased toughness.

Spent nuclear fuel (SNF) casks came into existence in the late 70's and early 80's of the 20th century when the fuel storage pools near reactor got overwhelmed their capacity and spent fuels are banned from recycling, hence had to transported through public route to destined geological

storage sites. Radiation from nuclear waste may causes human body cell death, genetic mutation, cancer, leukaemia, birth defects, and disorders of the reproductive, immune and endocrine systems. In order to avoid the leakage of radiation caused by sever accidental conditions during transportation and terrorist attacks the spent fuel containers should have sufficient toughness along with considerable strength. The functional requirements of these casks are (a) protect the SNF from accidental or fire damage; (b) provide shielding against radiation; (c) cool down the SNF to limit its peak cladding temperature; and (4) disposing waste packages (WPs). In last three decades investigations were carried out and reported all over the world to develop standard material for cask fabrication. Teng et.al, Jaksic and Nilsson [17, 18] used MSC/Dytran three dimensional programmes and continuum mechanics approach to solve this problem by the help of analytical methods. The test procedure consisted 1m drop impact test on flat undeformed concrete base and steel bar respectively to investigate the dynamic, nonlinear behaviour of SGCI full scale casks. The results obtained were well in agreement with the physically investigated results. Brynda et.al [19] reported the major criterion for fabricating SNF transportation and storage cask. They addressed three major investigations viz. structural integrity of cask, damage due to radiation situation and resistance to corrosion while loading the SNF and at climatic conditions of storage sites. Ductile iron and austenitic corrosion-resistant 1% boronated Cr-Ni steel were used for cask fabrication (1:2.5 scale) and tested for 9m drop impact test on the edge on a flat base and 1m flat drop impact on a spine protruding from flat base. It was concluded from the investigation that both the materials are suitable for the fabrication of SNF cask and meet the desired requirements. Besides these investigations on mechanical properties, fatigue response by addition of different alloying element and heat treatment application on ductile iron, as well as composites of ductile iron is studied and reported [20-23].

4

Previous study by many researchers was focused on the behavior of austempered ductile iron on mechanical as well as wear properties with respect to respective austempering condition and alloying elements. However for the specific purpose like spent nuclear fuel transportation very less number of works has been carried out and studies on behavior of annealed ductile iron is meager. Hence the current study is focused on comparison and correlation of microstructural aspects of annealed and austempered ductile iron aimed at to improve the toughness for spent nuclear fuel cask fabrication. In the current study attempt is also made to obtain higher amount of stable austenite at room temperature in order to improve the toughness of austempered ductile iron.

2. Experimental details

In order to carry out the investigation spheroidal graphite cast iron is made. The chemical composition in wt. % of the different ingots is presented in Table 1. Tensile and Izod impact test specimens were machined from the ingots following ASTM E8 & D256 standard respectively. To obtain the desired properties for nuclear fuel cask application, the tensile and impact specimens were austenitized at 1000°C for 90mins in Okay raising hearth furnace. Specimens are then cooled to 700°C and hold there for 5hr 30mins followed by furnace cooling to room temperature (to complete the annealing heat treatment process). On the other hand, for austempering, specimens were quenched in KNO_3+NaNO_3 (1:1 ratio) salt bath maintained at 500°C and hold there for 4hrs followed by air cooling to room temperature to obtain coarse upper bainitic matrix without retained austenite and carbide. The heat treatment processes are shown in Fig 1. The objective behind performing these two heat treatments is to get desired toughness of DI specimens for the application mentioned above. Prior to mechanical property determination the oxide layers from the specimens are removed by grinding process.

Table 1: chemical composition of ductile iron used in current study (in wt. %)

Alloy	Elements (in wt. %)											
	C	Si	Mn	S	P	Cr	Ni	Cu	Mo	Mg	Ce	Fe
LT-01	3.45	2.07	0.15	0.008	0.024	0.02	0.15	----	----	0.043	----	Rest
LT-2	3.61	2.10	0.20	0.007	0.022	0.03	0.47	0.009	0.001	0.043	0.004	Rest
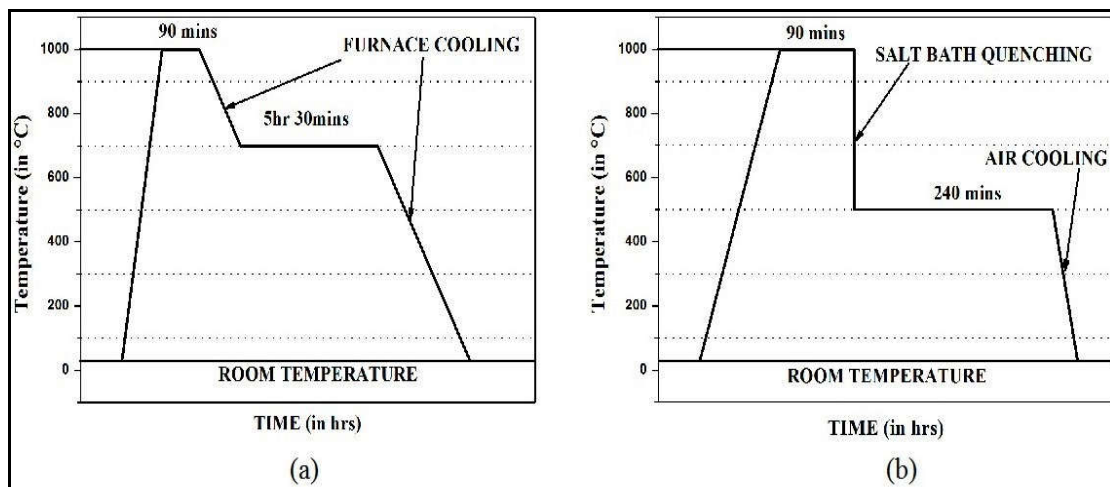
Fig. 1: Heat treatment processes employed in current study. (a) Annealing, (b) Austempering

Tensile strength, 0.2% yield strength and %elongation are determined by conducting tension test on INSTRON 1195 universal testing machine at a crosshead speed of 1mm/min. Vickers hardness (HV) is measured using Vickers hardness tester applying 20Kg load. VEEKAY - TL VS4 Izod impact tester was used for obtaining the impact energy, applying 21.7J hammer blow at a striking angle of 150°.

In order to detect the phases and crystallographic planes X-ray diffraction is carried out Rigaku - Ultima IV diffractometer using filtered Cu-Kα target (λ = 0.1542 nm) for a range of 40°-90° at scanning rate of 10°/min. The diffraction patterns are analyzed using Xpert Highscore

and JCPDS software. The volume fraction of austenite and ferrite in respective austempered specimens are calculated using the Direct Comparison Method [24], assuming only two phases i.e., austenite & ferrite were present in the matrix.

Metallographic investigation is carried out using image analyzer. Prior to the investigation, standard metallographic sample preparation technique was followed for each specimen and etched with 2% nital etch. Morphological aspects such as phase area fraction, nodularity and nodule count are determined following ASTM E2567-13a standard. Fracture phenomenon for each specimen after tensile and impact test is investigated by observing fracture surfaces under JEOL - JSM 6480LV, scanning electron microscope.

3. Results and discussion

According to the ASTM A874 Draft Specification Material Properties [25], the desired mechanical properties and microstructural aspects of DI material to be used for nuclear fuel transport cask are presented in Table 2.

Table 2: The desired mechanical properties and microstructural aspects of DI material to be used for nuclear fuel transport cask, according to ASTM A874 Draft Specification Material Properties.

Mechanical properties		Microstructure
UTS	45ksi (300MPa)	Essentially ferritic structure with no massive carbides.
YS	30ksi (200MPa)	> 90% type I and II graphite nodules.
Elongation	12%	< 275/mm2 graphite nodule count.
Static fracture toughness	50ksi-√inch (55MPa-√m)	

3.1 Specimen characterization

3.1.1 Morphological aspects

Microstructure of respective (annealed and austempered specimens) are shown in Fig. 2 and metallographic aspects such as nodularity, nodule count and area fraction of graphite, ferrite and bainite in respective specimens are presented in Table 3. Specimens subjected to annealing treatment developed fully ferritic matrix with nodular graphite embedded within, whereas the austempered specimens are found to have acicular upper baintic microstructure without martensite and zero carbide precipitation. The absence of martensite and zero carbide precipitation are attributed to the high austempering temperature i.e., 500°C and time (4hrs) which aggregate the increased carbon dissolution into austenite; consequently nullifying the transformation of carbide on subsequent cooling process [26]. The quantitative analysis also disclosed the formation of higher amount of bainite for alloy LT-2 which can be attributed to the presence of Mo, Cu (to a very little extent) and of higher amount of Si, Ni and Mn [27]. Further, presence of Mo, Cu and higher amount of Mn along with the aid of higher austempering temperature i.e., 500°C and austempering time (4hrs.) suppressed the formation of martensite or pearlite that normally appears when specimens cooled to room temperature in ambient atmosphere from austempering temperature [27-29]. The nodularity value appeared to decrease while nodule count increases in austempered specimen than that of the annealed specimens. This has been credited to the fact that, austempering involves a higher cooling rate that suppresses the carbon dissolution and consequently gives rise to more graphite nodule nucleation in the bainite matrix [30]. The effect of Cerium can't be ignored which resulted in higher (although minor in annealed specimen) nodule count (Table 3), for alloy LT-2 in both the heat treated condition. In annealed condition, LT-01 have higher ferrite area fraction than LT-2, whereas the latter has

8

higher bainite area fraction in austempered condition. At closer view it can be noticed that annealed specimens have different graphite size whereas that of in austempered specimens are almost same. This can be credited to the fact that annealing process involves slow diffusion process and doesn't show any significant change in graphite morphology as compared to as-cast specimen [31]. On the other hand austempering involves a rapid quenching process that suppresses the carbon dissolution and aggregates graphite nucleation sites.
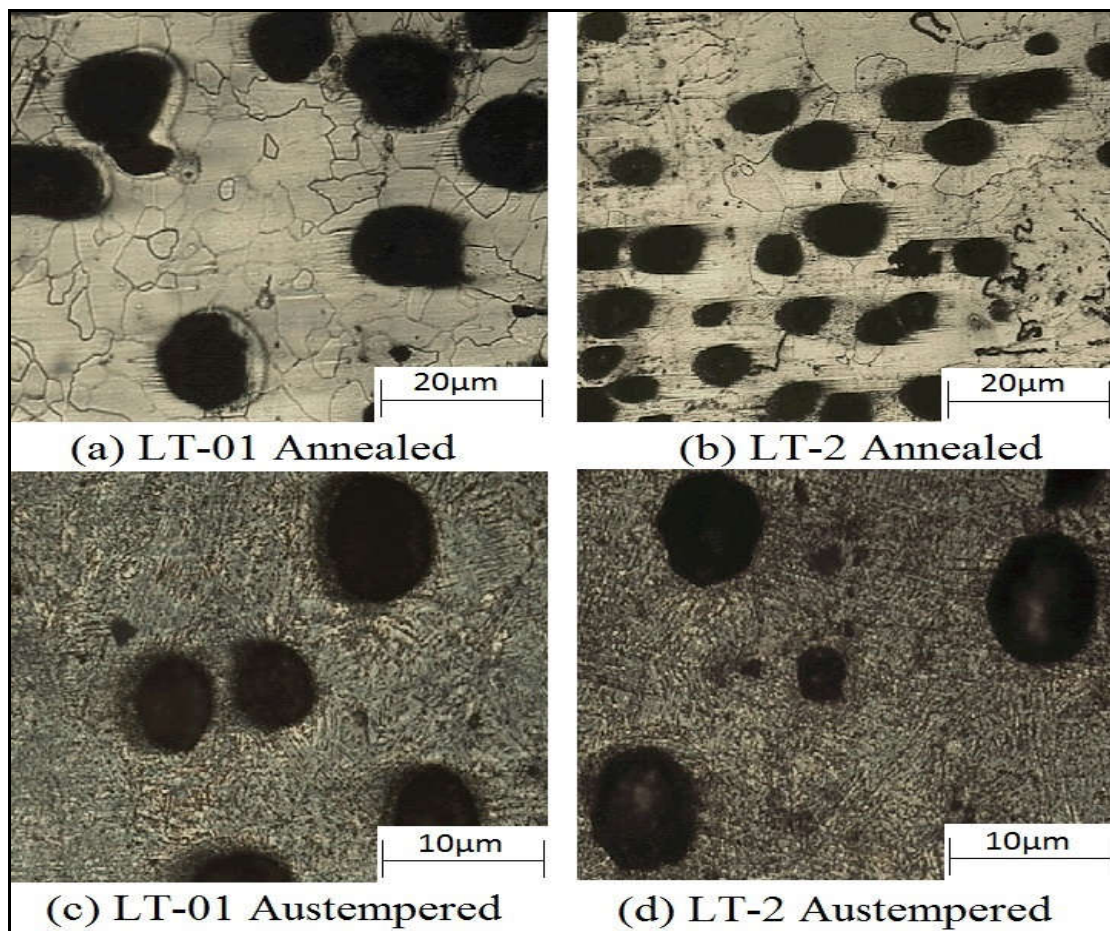
Fig. 2: Microstructure of respective specimens. (a) LT-01 Annealed at 100X, (b) LT-2 Annealed at 100X, (c) LT-01 Austempered at 200X, (d) LT-2 Austempered at 200X

Table 3: Morphological aspects of respective specimens

Specimen ID		Nodularity	Nodule count (mm^{-2})	Graphite area fraction	Bainite area fraction	Ferrite area fraction	Austenite volume fraction	Ferrite volume fraction
LT-01	Annealed	97%	23	20.5%	------	79.5%	------	------
	Austempered	81.5%	30	24.5%	75.5%	------	96%	4%
LT-2	Annealed	95.5%	25	25%	------	75%	------	------
	Austempered	88.5%	36	22%	78%	------	98.5%	1.5%

3.1.2   X-ray diffraction analysis

The X-ray diffraction patterns are presented in Fig. 3 for respective annealed and austempered specimens respectively. It is found that, the annealed specimens [Fig. 3 (a) & Fig. 3 (b)], showed BCC crystal structure whereas in austempered specimens [Fig. 3 (c) & Fig. 3 (d)], found to have both FCC & BCC crystallographic planes. This observation supports the presence of ferritic matrix microstructure for the annealed specimens and austempered specimens have bainitic matrix microstructure. Further, as bainitic matrix consists ferrite and Carbon enriched austenite, the carbon content of austenite in respective austempered specimens are calculated using the following equation.

$$a_\gamma = 0.3548 + 0.0044c_\gamma \text{ -------------- (1)}$$

Where a_γ is the lattice parameter of (311) austenitic peak in nanometer & c_γ is the corresponding carbon content in wt. %. The carbon content of LT-01 austempered specimen is found to be 2.14 wt.% and that of LT-2 was 2.24 wt.%, which is nearly about small difference in carbon wt.%.

Further the volume fraction of austenite and ferrite for respective austempered specimens were calculated using direct comparison method [23, 24], using equation (2) and equation (3) and the results are presented in Table 3. The attempt of producing ductile iron with higher amount of austenite was almost successful as was observed from the quantitative XRD analysis. The alloy LT-2 had achieved 98.5% austenite which was due to the higher amount of Ni, Si and Mn along with presence of Mo, Cu while LT-01 has 96% austenite. These high amounts of retained austenite are achieved by austempering at 500°C for 4hrs and are in complete agreement with the works of other authors [27-29].

$$\frac{I_\gamma}{I_\alpha} = \frac{R_\gamma}{R_\alpha} \times \frac{X_\gamma}{X_\alpha} \quad \text{------------ (2)}$$

$$X_\alpha + X_\gamma = 1 \quad \text{------------ (3)}$$

Where X_α and X_γ are the volume fraction, I_α and I_γ are the integrated intensities and R_α and R_γ are the theoretical relative intensity of the ferrite and austenite, respectively.
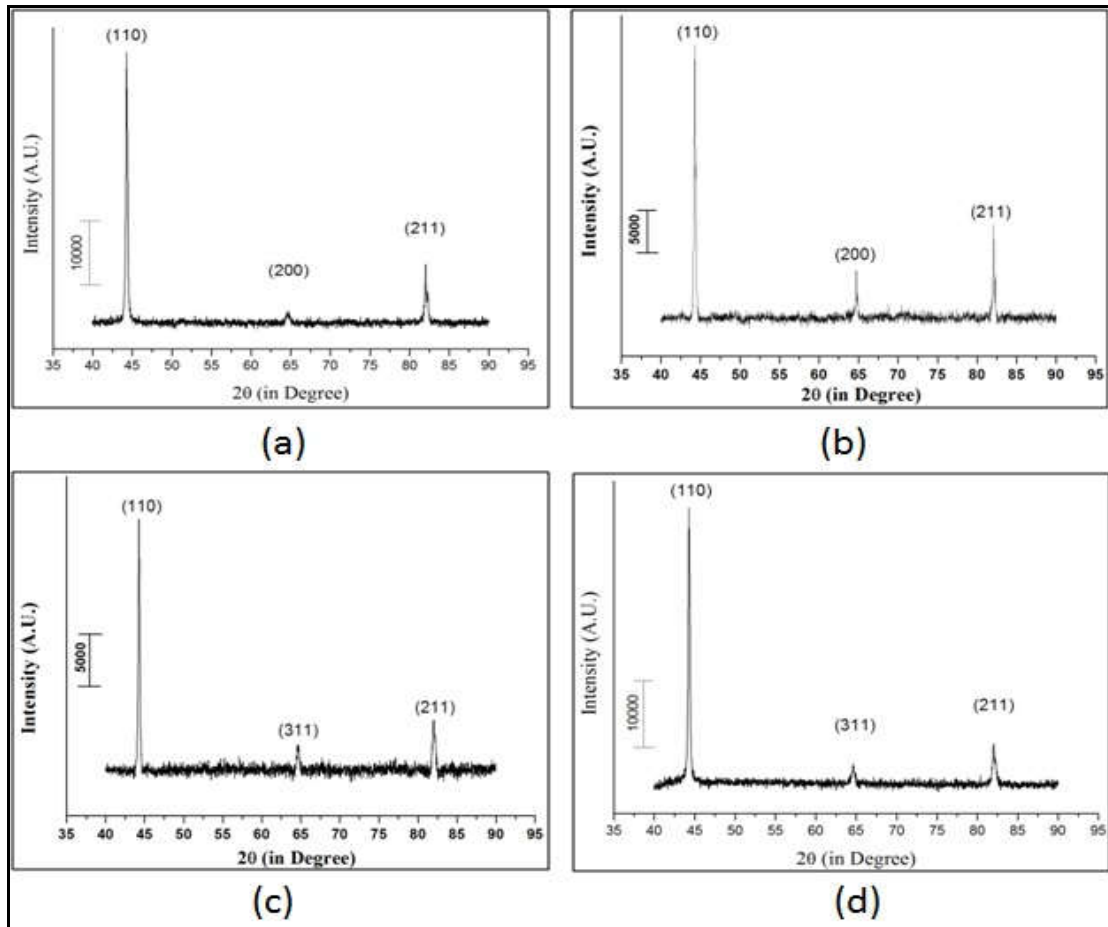
Fig. 3: XRD patterns of respective specimens. (a) LT-01 Annealed, (b) LT-2 Annealed,

(c) LT-01 Austempered, (d) LT-2 Austempered

3.2   Mechanical properties

Mechanical properties such as ultimate tensile strength, 0.2% proof stress, Vickers hardness and Izod impact energy are presented in Table 4. Annealed specimens appeared to be more ductile and tougher than those of respective austempered specimen due to the ferritic matrix which is the softest stable phase available at room temperature in Fe-C binary system [32]. At a closer view comparing both the alloys in annealing condition the Vickers hardness value of LT-2 was more than that of LT-01, although the latter was more ductile. The higher

12

ductility and impact resistance for LT-01 annealed specimen can be attributed to higher nodularity & ferrite area fraction evident from quantitative metallographic examination, Table 3. The higher hardness value of alloy LT-2 was due to the presence of higher Si content and addition of Mo, Cr & higher Ni content those provide strength to ferrite through solid solution strengthening [33]. This trend was also observed in case of austempered specimens. High strength values were found for both the alloys after austempering heat treatment leading to formation of upper bainitic matrix. The higher ductility value of alloy LT-2 austempered specimen can be attributed to increased nodularity value and higher Si and Cr content which promotes formation & stabilization of ferrite [34], whereas .02% proof stress was found to be lesser than that of alloy LT-01in both austempered and annealed condition. Presence of alloying elements viz. Mo, Cu and higher amount of Mn and Si resulted a significant increase in strength and hardness observed in austempered condition for alloy LT-2 in austempered condition [27, 35 and 36].

Table 4: Mechanical properties of both alloys subjected to annealing and austempering heat treatment process.

Alloy	Heat treatment	Mechanical properties				
		UTS (MPa)	0.2% YS (MPa)	% Elongation	Hardness (HV20)	Impact energy (J)
LT-01	Annealed	349.7	199.4	35.16%	124	33.35
	Austempered	783.9	434.3	11.35%	398	11.82
LT-2	Annealed	336.1	159.7	31.89%	220	29.75
	Austempered	842.5	356.7	14.11%	445	10.15

3.3   *Failure analysis*

Visual inspection under SEM reveals the failure phenomenon involved during the uniaxial tensile loading and Izod impact testing at ambient temperature for both the heat treatment conditions presented in Fig. 4 and Fig. 5 respectively. It can be seen that [Fig.4 (a) & (b) and Fig. 5(a) & (b)], that, the annealed specimens failed in ductile manner. The major feature that the presence of dimples which are formed due to microvoid coalescence phenomena confirms the ductile mode of failure and signifies the higher ductility and impact strength value. The *intergranular* fracture path is clearly observed around the nodules in ferritic planes which characterize the ductile mode of failure [37, 38]. On the other hand austempered specimens [Fig. 4 (c) & (d) and Fig. 5(c) & (d)], for both the alloys were failed mostly in brittle manner. The low energy stress paths referred as river marking is clearly visible in the bainitic matrix signifying brittle mode of failure. Also high strength and hardness of austempered specimens are justified by the presence of cleavage planes which are also major characteristic of brittle mode of failure.
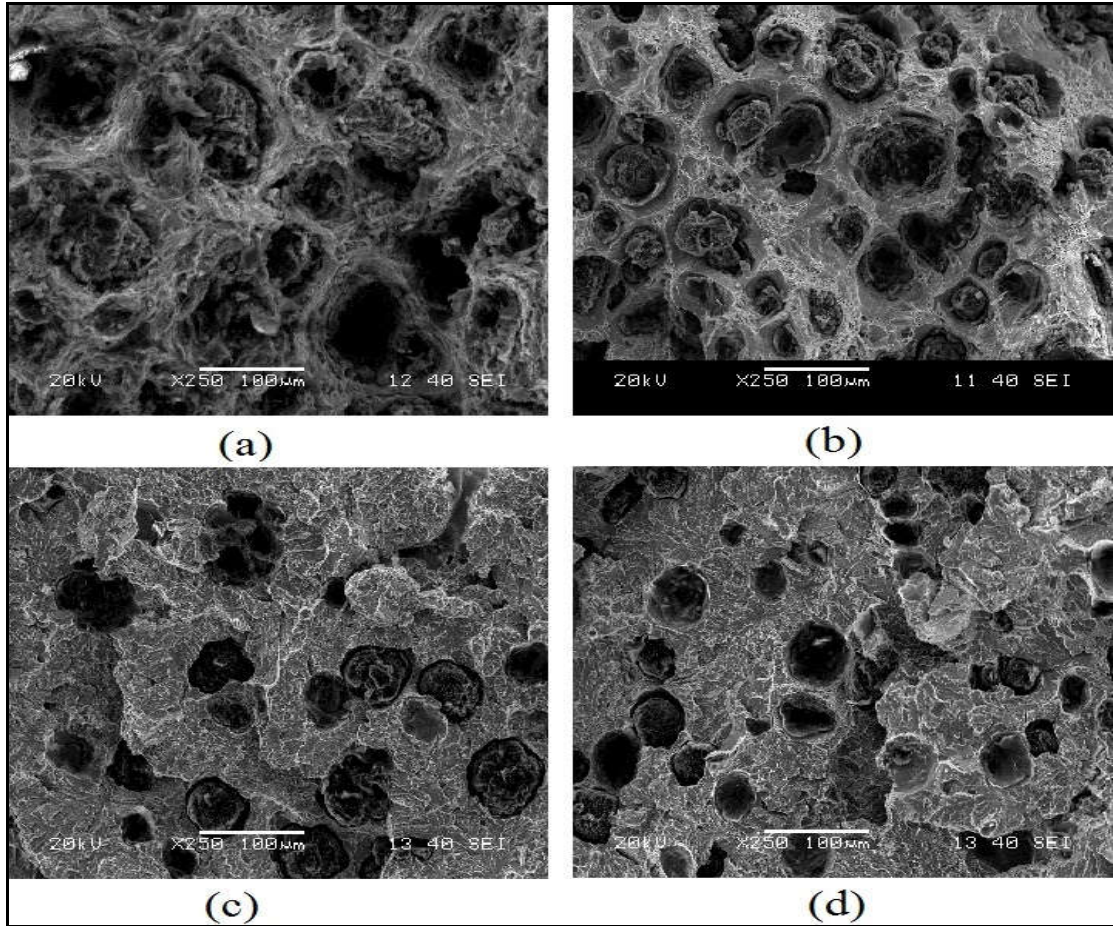
Fig. 4: Fractographs of respective specimens after tensile test. (a) LT-01 Annealed,

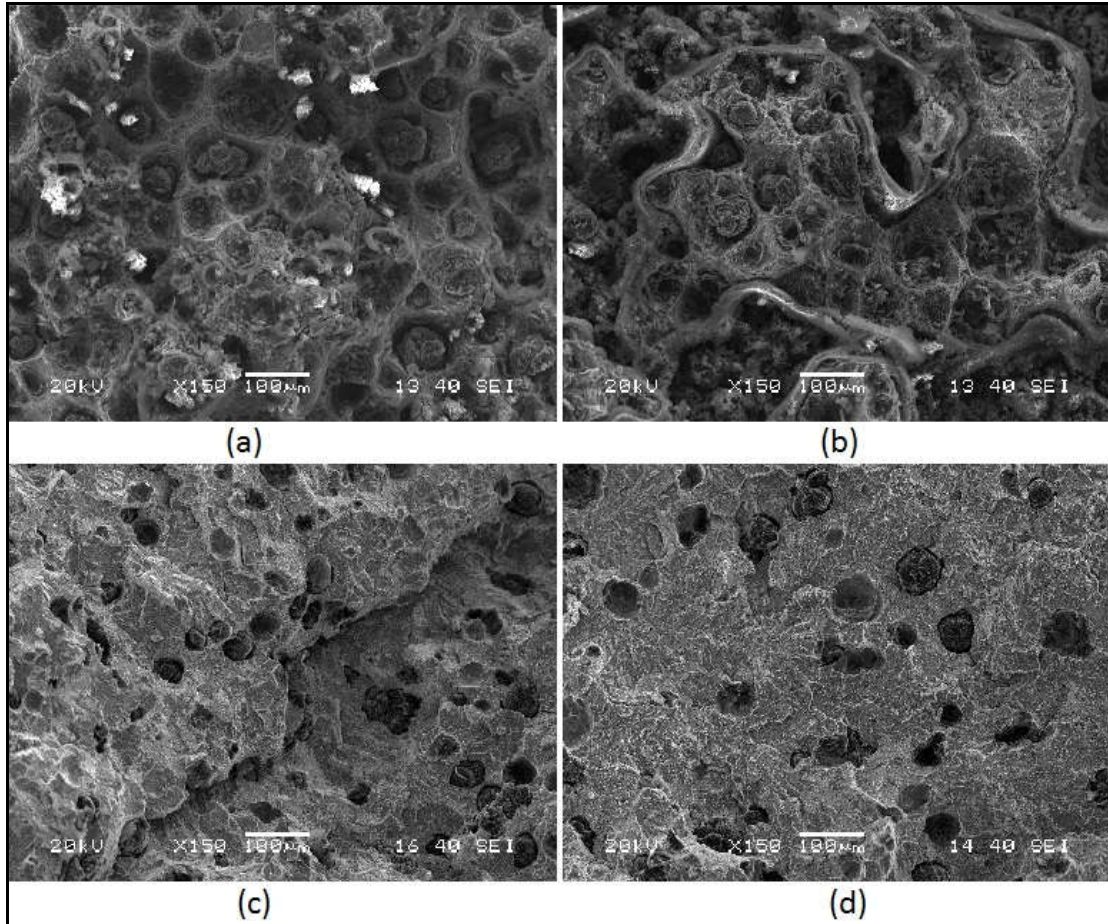(b) LT-2 Annealed, (c) LT-01 Austempered, (d) LT-2 Austempered

Fig. 5: Fractographs of respective specimens after impact test. (a) LT-01 Annealed,

(b) LT-2 Annealed, (c) LT-01 Austempered, (d) LT-2 Austempered

4.   Conclusion

In order to achieve desired properties (for spent nuclear fuel transport cask) ductile iron specimens are subjected to isothermal annealing and austempering heat treatments and the properties are correlated to microstructure. The following conclusions are drawn from this investigation.

1.   Isothermal annealing treatment led to production of graphite nodules embedded in fully ferritic matrix and austempering treatment on the other hand, produced ductile iron with

coarse upper baintic matrix with zero carbide due to higher austempering temperature and time of treatment.

2. The objective of achieving higher amount of austenite after austempering treatment is almost successful due to longer holding time at higher austempering temperature, leading to improved impact toughness.

3. Higher nodularity and ferrite area fraction led to increased ductility and impact resistance, whereas with increasing bainite area fraction resulted in increased tensile strength.

4. Effect of Mo, Cu and higher amount of Si, Cr and Ni in increasing the hardness through solid solution strengthening in ferritic ductile iron, and also increased bainite area fraction is observed.

5. Austempered specimens are observed to have better mechanical properties than ferritic specimens except higher elongation and impact energy in latter case, which are also evident from the fractographic analysis, showing ductile failure phenomena for annealed specimen and brittle mode of failure for austempered specimen.

6. The annealed specimens are proved to be appropriate for using in spent nuclear fuel transportation cask as the properties are well matched to the ASTM A874 Draft Specification, in both mechanical and microstructural requirements. On the other hand austempered specimens appeared to have strength values well above than the requirements.

5.   Acknowledgement

for providing test blocks for this investigation & M/S Steelage Engineering works, Rourkela, India for their immense help during machining of tensile and impact specimens.

6. References

1. R. Konečná, G. Nicoletto, L. Bubenko, S. Fintová, A comparative study of the fatigue behavior of two heat-treated nodular cast irons, Eng. Fract. Mech., 108 (2013), p.251–262.

2. R.C. Dommarco, M.E. Sousa, J.A. Sikora, Abrasion resistance of high nodule count ductile iron with different matrix microstructures, Wear, 257 (2004), p.1185–1192.

3. Ali M. Rashidi, M. Moshrefi-Torbati, Effect of tempering conditions on the mechanical properties of ductile cast iron with dual matrix structure (DMS), Mater. Lett., 45 (2000), p. 203–207.

4. Rong Zhou, Yehua Jiang, Dehong Lu, Rongfeng Zhou, Zhenhua Li, Development and characterization of a wear resistant bainite/martensite ductile iron by combination of alloying and a controlled cooling heat-treatment, Wear, 250 (2001), p.529–534.

5. R. Martins, J. Seabra, L. Magalhaes, Austempered ductile iron (ADI) gears: Power loss, pitting and micropitting, Wear, 264 (2008), p.838–849.

6. Olivera Eric, Milan Jovanovic, Leposava Sidanin , Dragan Rajnovic, Slavica Zec, The austempering study of alloyed ductile iron. Mater. and Des., 27 (2004), p.617–622.

7. Susil K. Putatunda, Sharath Kesani, Ronald Tackett, Gavin Lawes, Development of austenite free ADI (austempered ductile cast iron). Mater. Sci. and Eng. A, (2006), p.435–436.

8. K. Narasimha Murthy, P. Sampathkumaran, S. Seetharamu, Abrasion and erosion behaviour of manganese alloyed permanent moulded austempered ductile iron, Wear, 267 (2009), p.1393–1398.

9. Z. M. El-Baradie, M. M. Ibrahim, I. A. El-Sisy, and A. A. Abd El-Hakeem, AUSTEMPERING OF SPHEROIDAL GRAPHITE CAST IRON, Mater. Sci., 40 (2004), No. 4, p.523-528.

10. Murat Baydogan , Seckin Izzet Akray , Successive Boronizing and Austempering for GGG-40 Grade Ductile Iron, J. OF IRON AND STEEL RES. INT., 16 (2009), No.2, p.50-54.

11. A.R. Ghaderi, M. Nili Ahmadabadi, H.M. Ghasemi, Effect of graphite morphologies on the tribological behavior of austempered cast iron, Wear, 255 (2003), p.410–416.

12. Peng Yun-Cheng, Jin Hui-Jin, Liu Jin-Hai, Li Guo-Lu, Influence of cooling rate on the microstructure and properties of a new wear resistant carbidic austempered ductile iron (CADI), MATER. CHARACT., 72 (2012), p.53 – 58.

13. Susil K. Putatunda, Comparison of the Mechanical Properties of Austempered Ductile Cast Iron (ADI) Processed by Conventional and Step-Down Austempering Process, Mater. and Manuf. Process., 25 (2010), p.749–757.

14. Yun-Cheng Peng, Hui-Jin Jin, Jin-Hai Liu, Guo-Lu Li, Effect of boron on the microstructure and mechanical properties of carbidic austempered ductile iron, Mater. Sci. and Eng. A, 529 (2011), p.321– 325.

15. L. SIDJANIN, R. E. SMALLMAN and J. M. YOUNG, ELECTRON MICROSTRUCTURE AND MECHANICAL PROPERTIES OF SILICON AND ALUMINIUM DUCTILE IRONS, Acta metall. & mater., 42 (1994), No.9, p.3149-3156.

16. Ayman H. Elsayed, M.M. Megahed, A.A. Sadek, K.M. Abouelela, Fracture toughness characterization of austempered ductile iron produced using both conventional and two-step austempering processes, Mater. and Des., 30 (2009), p.1866–1877.

17. T.L. Teng, Y.A. Chu, F.A. Chang, H.S. Chin, M.C. Lee, The dynamic analysis of nuclear waste cask under impact loading, Annals of Nuclear Energy, 30 (2003), p.1473–1485.

18. Nikola Jaksic, Karl-Fredrik Nilsson, Finite element modelling of the one meter drop test on a steel bar for the CASTOR cask, Nuclear Engineering and Des., 239 (2009), p.201–213.

19. Jiri Brynda, Pavel Hosnedl, Miroslav Jilek and Miroslav Picek, Material Issues in Manufacturing and Operation of Transport and Storage Spent Fuel Casks, Transactions of 15th International Conference on Structural Mechanics in Reactor Technology, 1999, p.247-253.

20. M. Kazemi, A.R. Kiani-Rashid, A. Nourian, A. Babakhani, Investigation of microstructural and mechanical properties of austempered steel bar-reinforced ductile cast iron composite, Mater. and Des., 53 (2014), p.1047–1051.

21. Cristiana Delprete, Raffaella Sesana, Experimental characterization of a Si–Mo–Cr ductile cast iron, Mater. and Des., 57 (2014), p.528–537.

22. A.Alhussein, M.Risbet, A.Bastien, J.P.Chobaut, D.Balloy, J.Favergeon, Influence of silicon and addition elements on the mechanical behavior of ferritic ductile cast iron, Mater. Sci. & Eng. A, 605 (2014), p.222–228.

23. Cheng-Hsun Hsu, Kuan-Ting Lin, A study on microstructure and toughness of copper alloyed and austempered ductile irons, Mater. Sci. and Eng. A, 528 (2011), p.5706–5712.

24. B.D.Culity, ELEMENTS OF X-RAY DIFFRACTION, ADDISON-WESLEY PUBLISHING COMPANY, INC., MASSACHUSETTS, 1956.

25. Ken B. Sorenson, Richard J. Salzbrenner, QUALITY ASSUARANCE ASPECTS IN USING DUCTILE CAST IRON FOR TRANSPORTATION CASKS, WMS papers, Phoenix, 1988, 107.

26. M. Heydarzadeh Sohi, M. Nili Ahmadabadi, A. Bahrami Vahdat, The role of austempering parameters on the structure and mechanical properties of heavy section ADI, J. of Mater. Process. Technol., (2004), p.203–208.

27. W. Xu, M. Ferry, Y. Wang, The effect of ausferrite formation on the mechanical properties of gray iron, Scr. Mater., 51 (2004), p.705–709.

28. O. Eric, L. Sidjanin, Z. Miskovic, S. Zec, M.T. Jovanovic, Microstructure and toughness of CuNiMo austempered ductile iron, Mater. Lett., 58 (2004), p.2707 – 2711.

29. J.M. Han, Q. Zou, G.C. Barber, T. Nasir, D.O. Northwood, X.C. Sun, P. Seaton, Study of the effects of austempering temperature and time on scuffing behavior of austempered Ni–Mo–Cu ductile iron, Wear, 290–291 (2012) p.99–105.

30. N. Rebasa, R. Dommarco, J. Sikora, Wear resistance of high nodule count ductile iron, Wear, 253 (2002), p.855–861.

31. Yufu Sun, Sumeng Hu, Zhiyun Xiao, Sansan You, Jingyu Zhao, Yezhe Lv, Effects of nickel on low-temperature impact toughness and corrosion resistance of high-ductility ductile iron, Mater. and Des., 41 (2012) p.37–42.

32. E.M. El-Banna, A study of ferritic centrifugally cast ductile cast iron, Mater. Lett., 20 (1994), p.99- 106.

33. G.S.Cho, K.H.Choe, K.W.Lee and A.Ikenaga, Effects of Alloying Elements on the Microstructures and Mechanical Properties of Heavy Section Ductile Cast Iron, J. of Mater. Sci. and Technol., 23 (2007), No.1, p.97-101.

34. R.A. Gonzaga, Influence of ferrite and pearlite content on mechanical properties of ductile cast irons, Mater. Sci. & Eng. A, 567 (2013), p.1–8.

35. P.W. Shelton, A.A. Bonner, The effect of copper additions to the mechanical properties of austempered ductile iron (ADI), J. of Mater. Process. Technol., 173 (2006), p.269–274.

36. B.Y. Lin, E.T. Chen, T.S. Lei, THE EFFECT OF ALLOY ELEMENTS ON THE MICROSTRUCTURE AND PROPERTIES OF AUSTEMPERED DUCTILE IRONS, Scr. Metall. et Mater., 32 (1995), No.9, p.1363-1367.

37. Victor Kerlins, ASM Handbook, edited by Kathleen Mills, Joseph R. Davis, James D. Destefani, Deborah A. Dieterich, Heather J. Frissell, George M. Crankovic, Diane M. Jenkins (Eds.), ASM International, USA, 1987, p.12-14.

38. S. SEN, S. C. MISHRA & S. SARKAR, CHARACTERIZATION OF ADI THROUGH FRACTOGRAPHIC ANALYSIS, THE TECHNOL. WORLD QUARATELY J., V (2010), No.1, p.45-48.

List of figures:

List of tables: